Influence of Gas Feed Composition and Pressure on the Catalytic Conversion of CO_2 to Hydrocarbons Using a Traditional Cobalt-Based Fischer−Tropsch Catalyst

Robert W. Dorner,[†] Dennis R. Hardy,[†] Frederick W. Williams,[†] Burtron H. Davis,[‡] and Heather D. Willauer*[,†]

Naval Research Laboratory, Code 6180, Navy Technology Center for Safety and Survivability Branch, 4555 Overlook Avenue, SW, Washington, D.C. 20375, and Center for Applied Energy Research, 2540 Research Park Drive, Lexington, Kentucky 45011

Received March 30, 2009. Revised Manuscript Received May 22, 2009

The hydrogenation of CO_2 using a traditional Fischer−Tropsch Co−Pt/Al_2O_3 catalyst for the production of valuable hydrocarbon materials is investigated. The ability to direct product distribution was measured as a function of different feed gas ratios of H_2 and CO_2 (3:1, 2:1, and 1:1) as well as operating pressures (ranging from 450 to 150 psig). As the feed gas ratio was changed from 3:1 to 2:1 and 1:1, the production distribution shifted from methane toward higher chain hydrocarbons. This change in feed gas ratio is believed to lower the methanation ability of Co in favor of chain growth, with possibly two different active sites for methane and C_2−C_4 products. Furthermore, with decreasing pressure, the methane conversion drops slightly in favor of C_2−C_4 paraffins. Even though under certain reaction conditions product distribution can be shifted slightly away from the formation of methane, the catalyst studied behaves like a methanation catalyst in the hydrogenation of CO_2.

1. Introduction

The U.S. Department of Defense (DOD) is the single largest buyer and consumer of fuel, using approximately 12.6 million gallons per day.[1] Approximately 11 million gallons per day is jet fuel (note the term jet fuel includes use in both aircraft and ground vehicles), and the remainder is shipboard marine distillate (all Navy and Marine Corps use). The Defense Energy Support Center reports a 2008 fuel cost per gallon of $4 dollars; this amounts to a total cost to the DOD of over $18 billion annually. Additional costs are acquired in the logistical procurement and delivery of the fuel.[1]

World-wide "peak oil" production is expected to occur from 2010 to 2025+ (by some experts estimate that we have already reached peak production since 2004).[2] This along with increasing demand can cause large swings in price and availability. Fuel independence would alleviate uncertainties in the world market supply of oil along with commercial fluctuations in price. In addition only high energy density petroleum-derived fuel meets stringent military aviation requirements.[3] Thus, the DOD has a vested interest in maintaining this supply by supporting the development of synthetic hydrocarbon fuel from the vast natural resources, such as coal, shale, gas hydrates, and CO_2, available in the United States.[4]

Given sufficient primary energy resources, such as coal and natural gas, technologies currently exist to synthesize hydrocarbon fuel.[3] Sasol is the single largest company that has designed, built, and currently operates Fischer−Tropsch (FT) processes in South Africa and Qatar. The Qatar plant produces 34 000 barrels of product a day using natural gas as its carbon and hydrogen source.[5] A total of 70% of the product is wax that is refined to diesel fuel by Chevron, and the other 30% is gasoline and diesel fuel. The South Africa plant produces 160 000 barrels of product a day by steam-reforming coal to generate syngas for the FT process.[5] A water−gas shift is needed to obtain a 2:1 ratio of hydrogen/carbon monoxide. The final product is jet and diesel fuel. Shell also has an operating gas to liquids (GTL) plant in Bintulu, Malaysia. The plant opened in 1993 and was producing 14 700 barrels per day in 2005 of liquid hydrocarbon products.

Since the end of World War II (in 1945), advances in catalyst development and reactor engineering have made the FT process significantly more efficient.[6] However, these technologies are not CO_2-neutral, and they are only practical for land-based applications. As a result, there is still a need for more favorable and cost-effective methods of synthesizing fuel from other natural resources.[3]

The ocean represents an important resource with regard to its total carbon content. For example, CO_2 is relatively

* To whom correspondence should be addressed: Naval Research Laboratory, Chemistry Division, Code 6180, 4555 Overlook Ave., SW, Washington, D.C. 20375. E-mail: heather.willauer@nrl.navy.mil.

[†] Naval Research Laboratory.

[‡] Center for Applied Energy Research.

(1) Petroleum Quality Information System Report. Defense Energy Support Center (DESC) BP, Fort Belvoir, VA, 2008.

(2) Roberts, P. *National Geographic* June **2008**.

(3) Coffey, T.; Hardy, D. R.; Besenbruch, G. E.; Schultz, K. R.; Brown, L. C.; Dahlburg, J. P. *Def. Horiz.* **2003**, *36*, 1.

(4) Olah, G. A.; Goeppert, A.; Prakash, G. K. S. *Beyond Oil and Gas: The Methanol Economy*; Wiley-VCH Verlag GmbH and Co. KGaA: Weinheim, Germany, 2006.

(5) Davies, P. Introduction and overview. http://www.sasol.com/sasol_internet/downloads/1_PatDavies_Welcome_1109332901579.pdf (accessed August 2008).

(6) Davis, B. H. *Top. Catal.* **2005**, *32*, 143–168.

10.1021/ef900275m

Report Documentation Page

Form Approved
OMB No. 0704-0188

1. REPORT DATE	2. REPORT TYPE	3. DATES COVERED
2009		**00-00-2009 to 00-00-2009**

4. TITLE AND SUBTITLE	5a. CONTRACT NUMBER
Influence of Gas Feed Composition and Pressure on the Catalytic Conversion of CO2 to Hydrocarbons Using a Traditional Cobalt-Based Fischer-Tropsch Catalyst	5b. GRANT NUMBER
	5c. PROGRAM ELEMENT NUMBER
6. AUTHOR(S)	5d. PROJECT NUMBER
	5e. TASK NUMBER
	5f. WORK UNIT NUMBER
7. PERFORMING ORGANIZATION NAME(S) AND ADDRESS(ES) **Naval Research Laboratory,Code 6180, Navy Technology Center for Safety and Survivability Branch,4555 Overlook Avenue, SW,,Lexington,KY,45011**	8. PERFORMING ORGANIZATION REPORT NUMBER
9. SPONSORING/MONITORING AGENCY NAME(S) AND ADDRESS(ES)	10. SPONSOR/MONITOR'S ACRONYM(S)
	11. SPONSOR/MONITOR'S REPORT NUMBER(S)

12. DISTRIBUTION/AVAILABILITY STATEMENT
Approved for public release; distribution unlimited

13. SUPPLEMENTARY NOTES

14. ABSTRACT

15. SUBJECT TERMS

16. SECURITY CLASSIFICATION OF:			17. LIMITATION OF ABSTRACT	18. NUMBER OF PAGES	19a. NAME OF RESPONSIBLE PERSON
a. REPORT **unclassified**	b. ABSTRACT **unclassified**	c. THIS PAGE **unclassified**	**Same as Report (SAR)**	**6**	

concentrated at approximately 100 mg/L of seawater.[7,8] The $[CO_2]_T$, as shown in eq 1, is the sum of the concentration of dissolved gaseous CO_2, bicarbonate, and carbonate.

$$\sum [CO_2]_T = [CO_2(g)] + [HCO_3^-] + [CO_3^{2-}] \qquad (1)$$

In the equation, $[CO_2\ (g)]$ is about 2−3% of the total CO_2 content in seawater, the dissolved carbonate is about 1%, and the remainder is bicarbonate.[9] This concentration is about 140 times greater than that found in air.[3] The $[CO_2]_T$ in air is 370 ppm (v/v), and this is only 0.7 mg/L (w/v) compared to the 100 mg/L in the ocean.[3] Thus, if CO_2 could economically be extracted from the ocean, then marine engineering processes could be envisioned to use this carbon source as a potential chemical feedstock.[10,11] From an environmental perspective, such a process would have tremendous benefits in reducing the impact of anthropogenic CO_2 on climate change and would eliminate the emission of sulfur and nitrogen compounds that are readily produced from the combustion of petroleum-derived fuels.[2]

The problem with the use of CO_2 is its great chemical stability. One of the few avenues open for chemical reaction is that with hydrogen. The following enthalpies of formation describe (a) the direct hydrogenation of CO_2 to HC and (b) the reverse water−gas shift reaction (RWGS), followed by (c) the conversion of CO to hydrocarbons via a FT mechanism:[11]

$$\text{(a) } CO_2 + 3H_2 \rightarrow (CH_2) + 2H_2O \quad \Delta_R H_{300\,^\circ C} = -128 \text{ kJ/mol}$$

$$\text{(b) } CO_2 + H_2 \rightarrow CO + H_2O \quad \Delta_R H_{300\,^\circ C} = +38 \text{ kJ/mol}$$

$$\text{(c) } CO + 2H_2 \rightarrow (CH_2) + H_2O \quad \Delta_R H_{300\,^\circ C} = -166 \text{ kJ/mol}$$

In the reactions, (a) direct conversion of CO_2 and the conversion of CO_2 to HC via the (b) RWGS and (c) subsequent chain growth are overall exothermic and, thus, a feasible route to converting CO_2 to hydrocarbons. Although it must be noted that methane is thermodynamically the most favored HC product.[12] However, very little research has been performed applying CO_2 as the carbon source, because generally CO_2 has been thought of as having too high of an energy barrier for polymerization, even in the presence of a catalyst. Souma and co-workers evaluated various composite catalysts for hydrogenation of CO_2 to alcohols and hydrocarbons.[13−17] Composite catalysts composed of iron, zinc, zeolite, and zirconium were highly selective for the production of isobutene and branched C_{5+} hydrocarbons.[14] Davis and co-workers have looked at the conversion of CO/H_2, CO_2/H_2, and $(CO + CO_2)/H_2$ mixtures in a fixed-bed synthesis using cobalt catalysts.[14] They concluded that CO and CO_2 hydrogenation occur at the same rate but follow different reaction pathways because of the difference in product formation. Approximately 70% more methane was formed in the hydrogenation of CO_2,[15] with an expected equilibrium conversion of 50%.[17] When experiments were conducted with an iron catalyst, the conversion of CO_2 was found to be much lower than the conversion of CO.[17−19]

CO_2 represents an abundant carbon resource. Its potential as a chemical feedstock for the production of valuable hydrocarbons is of great interest. Having shown the ability to convert CO_2 to hydrocarbons,[13−19] the objective of this study was to change experimental conditions to improve the production distribution toward higher chain hydrocarbons (HCs) and increase conversion rates of traditional FT cobalt catalysts.

2. Experimental Section

Catalyst Preparation. Co−Pt/γ-Al_2O_3 with a surface area, pore volume, and pore radius of 130 m^2/g, 0.28 cm^3/g, and 3.82 nm, respectively, was used as support material. Alumina was chosen over SiO_2 because it increases metal dispersion as well as prevents catalyst sintering. A multi-step incipient wetness impregnation method was used to add cobalt nitrate hexahydrate $[Co(NO_3)_2 \cdot 6H_2O]$ solution to alumina. The support was initially impregnated with 12.5 wt % Co and subsequently dried under vacuum at 90 °C using a rotary evaporator. The solid was dried at 110 °C in static air, and the procedure was repeated, obtaining a cobalt loading of 25 wt %. Between each step, the catalyst was dried under vacuum in a rotary evaporator at 90 °C for 2 h. After the cobalt addition, 0.5 wt % Pt was impregnated using platinum tetrachloride ($PtCl_4$). The catalyst was then dried at 110 °C in static air and subsequently calcined at 400 °C for 6 h under flowing air (10 slph).

Characterization. Brunauer−Emmett−Teller (BET) surface area measurements were conducted using a Micromeritics Tri-Star system. An appropriate amount (∼0.25 g) of catalyst sample was taken and slowly heated to 160 °C for 10 h under vacuum (∼50 m Torr). The sample was then transferred to the adsorption unit, and the N_2 adsorption was measured at the boiling temperature of nitrogen.

Continuously Stirred Tank Reactor (CSTR) Synthesis. CO_2 hydrogenation reactions were conducted in a 1 L three-phase slurry CSTR. In a typical experiment, 12−15 g of calcined 0.5% Pt−25% Co/γ-Al_2O_3 catalyst (80−140 mesh) was reduced *ex situ* using a H_2/He (1:3) mixture at 350 °C for 10 h. The reduced catalyst was transferred to a 1 L CSTR, which already contained 310 g of melted Polywax 3000 under flowing nitrogen. The catalyst was reduced *in situ* using pure H_2 (15 slph) for 24 h at 230 °C. Three Brooks mass flow controllers were used to control the flow rate of CO_2, H_2, and N_2. Hydrogenation of CO_2 was conducted at 220 °C, 275 psig, and a constant space velocity of 4.0 SL h^{-1} g^{-1} of catalysts with different H_2/CO_2 ratios (3:1, 2:1, and 1:1). In another set of experiments, the H_2/CO_2 ratio was kept constant (3:1), and the reactor pressure was varied from 150 to 450 psig. The effluent gases were analyzed online using a Micro gas chromatograph (GC) equipped with a Porapak Q packed column and thermal conductivity detector (TCD), with the TCD temperature set to 110 °C and the

(7) Takahashi, T.; Broecker, W. S.; Bainbridge, A. E. *The Alkalinity and Total Carbon Dioxide Concentration in the World Oceans in Carbon Cycle Model*; SCOPE: New York, 1981; Vol. 16, pp 271−286.
(8) Takahashi, T.; Broecker, W. S.; Werner, S. R.; Bainbridge, A. E. *Carbonate Chemistry of the Surface of the Waters of the World Oceans in Isotope Marine Chemistry*; Goldberg, E. D., Horibe, Y., Katsuko, S., Eds.; Uchida Rokakuho: Tokyo, Japan, 1980; pp 291−326.
(9) Werner, S.; Morgan, J. J. *Aquatic Chemistry: An Introduction Emphasizing Chemical Equilibrium in Natural Waters*; Wiley-Interscience: New York, 1970.
(10) Hardy, D. R.; Zagrobelny, M.; Willauer, H. D.; Williams, F. W. Extraction of carbon dioxide from seawater by ion exchange resin. Part I: Using a strong acid cation exchange resin. NRL Memorandum Report 6180-07-9044, April 20, 2007.
(11) Willauer, H. D.; Hardy, D. R.; Lewis, M. K.; Williams, F. W. Recovery of $[CO_2]_T$ from aqueous bicarbonate using a gas permeable membrane. NRL Memorandum Report 6180-08-9129, June 25, 2008.
(12) Riedel, T.; Schaub, G.; Jun, K.-W.; Lee, K.-W. *Ind. Eng. Chem. Res.* **2001**, *40*, 1355–1363.
(13) Fujiwara, M.; Kieffer, R.; Ando, H.; Souma, Y. *Appl. Catal., A* **1995**, *121*, 113–124.
(14) Kieffer, R.; Fujiwara, M.; Udron, L.; Souma, Y. *Catal. Today* **1997**, *36*, 15–24.
(15) Fujiwara, M.; Kieffer, R.; Ando, H.; Xu, Q.; Souma, Y. *Appl. Catal., A* **1997**, *154*, 87–101.
(16) Tan, Y.; Fujiwara, M.; Ando, H.; Xu, O.; Souma, Y. *Ind. Eng. Chem. Res.* **1999**, *38*, 3225–3229.
(17) Zhang, Y.; Jacobs, G.; Sparks, D. E.; Dry, M. E.; Davis, B. H. *Catal. Today* **2001**, *71*, 411–418.
(18) Xu, L.; Bao, S.; Houpt, D. J.; Lambert, S. H.; Davis, B. H. *Catal. Today* **1997**, *36*, 347–355.
(19) Riedel, T.; Claeys, M.; Schulz, H.; Schaub, G.; Nam, S.-S.; Jun, K.-W.; Choi, M.-J.; Kishan, C.; Lee, K.-W. *Appl. Catal., A* **1999**, *186*, 201–213.

Table 1. Sample Conditions at 275 psi and 220 °C

		feed in (SLPH)		feed out (SLPH)		conversion (%)	conversion (%)
ratio	TOS (h)	H_2	CO/CO_2	H_2	CO/CO_2	H_2	CO/CO_2
	33.5	22.0	10.4	6.3	3.0	71.4	71.4
	57.7	22.0	10.4	8.4	4.1	61.6	60.9
	83.3	22.0	10.4	10.1	4.9	53.9	52.8
2:1 H_2/CO	107.5	22.0	10.4	11.2	5.4	49.1	48.0
	157.3	22.0	10.4	11.4	5.5	48.4	47.2
	178.8	22.0	10.4	11.6	5.6	47.1	46.0
	203	22.0	10.4	11.6	5.6	47.5	45.8
	226	30.6	9.1	16.8	5.4	45.2	40.0
	249	30.6	9.1	17.1	5.5	44.3	38.8
	278	30.6	9.1	17.8	5.7	41.9	37.4
3:1 H_2/CO_2	323	30.6	9.1	17.5	5.6	42.9	38.1
	346	30.6	9.1	18.3	5.8	40.4	35.8
	371	30.6	9.1	19.1	6.1	37.8	32.9
	393	30.6	9.1	19.5	6.2	36.4	31.1
	417	20.8	9.0	12.3	6.5	40.7	27.9
	444	20.8	9.0	12.6	6.6	39.3	26.3
2:1 H_2/CO_2	494	20.8	9.0	12.7	6.6	38.7	26.2
	514	20.8	9.0	12.8	6.5	38.6	27.2
	538	20.8	9.0	12.9	6.6	38.0	26.5
	753	10.8	10.8	6.9	10.1	36.5	6.5
	784	10.8	10.8	7.1	10.0	34.4	7.9
1:1 H_2/CO_2	836	10.8	10.8	7.3	10.2	32.8	5.7
	880	10.8	10.8	7.3	9.9	32.0	8.1
	1000	10.8	10.8	8.1	10.1	25.2	6.8
2:1 H_2/CO	1048	21.7	10.8	16.3	8.1	24.9	25.4
	1072	21.7	10.8	16.5	8.2	23.8	24.1

GC column oven set to 70 °C. The GC was calibrated using a mixture of gases with known molar ratio. Several calibration runs were preformed, and an average was taken prior to catalysis testing. With the current instrumental configuration, it was not possible to quantify the water content in the effluent.

3. Results and Discussion

Data were collected on the conversion of CO and CO_2 over the Co−Pt/γ-Al_2O_3 catalyst for 1072 h. A second run was performed to corroborate the initial data collected. After having the catalyst on stream for 226 h, the feedstock gas composition is changed, with CO_2 replacing CO, to measure the CO_2 hydrogenation ability of the catalyst. During initial data acquisition, the gas ratio of $CO/H_2/N_2$ is 1:2:1 and yields, as expected, mainly higher chain HCs. The initial conversion rate of CO to HC is, as expected, high but reaches steady state after approximately 200 h on stream, as can be seen in Table 1. CO is selected as the initial reactant to obtain steady state in reaction conditions before switching to CO_2 as the feed gas (see Table 1 for reaction conditions and Table 2 for product distribution). When the feed gas is switched to CO_2, the initial conversion rate falls from 46% for the syngas to 40% (Table 1). The rate of both CO_2 and H_2 consumption continues to decline during the following 1000 h on stream by approximately 86 and 37% (Table 1). This drop in the conversion rate may be attributed to the deactivation of the catalyst with time-on-stream (TOS) rather than a result of the change in feed gas composition. This is shown by the fact that, when switching back to CO in the feed gas after 1000 h, a marked drop is observed in the syngas conversion rates (around 24%; Table 1) in comparison to the initial rates obtained over a fresh catalyst.

Table 2 shows that, when CO_2 is part of the feed gas (with a ratio of $H_2/CO_2 = 3:1$), the main product formed is methane (97.6% C). In an effort to shift product distribution away from methane toward longer chain HCs, the ratio of H_2/CO_2 was changed from 3:1 to 2:1 (using N_2 as the inert gas equaling the volume of CO_2) and subsequently 1:1. Besides the feed gas ratio, the remaining experimental conditions were kept constant. Interestingly, the portion of longer chain HC (i.e., HC above methane) increases with increasing TOS, irrespective of the H_2/CO_2 ratio (i.e., between 753 and 1000 h TOS at a constant H_2/CO_2 ratio equaling 1:1; see Table 2). The product distribution throughout the experiment however highly favors methane as the main product. It was possible to obtain a larger fraction of C_2-C_4 products though (up to 6.9% at H_2/CO_2 equaling 1:1) upon reducing the H_2 concentration in the feed gas (Table 1). Olefin production was negligible (Table 2); however, when changing the H_2/CO_2 ratio to 1:1, it is possible to slightly increase the amount of olefins produced. This occurrence most likely originates from the lack of H_2 present in the feed gas, and thus, olefin production becomes more favorable.

As the H_2 consumption in the feed gas drops throughout the experiment from 45.19 to 28.58%, the CO_2 conversion is reduced from 40.03 to 5.56% (see Table 1). Overall, the best C_2-C_4/methane ratio was obtained, when switching to a 1:1 H_2/CO_2 feed gas ratio. Concomitantly to the drop in methane selectivity when reducing the H_2 content in the gas, the overall conversion of the catalyst drops; however, as pointed out earlier, this is most likely due to deactivation of the catalyst with increasing TOS.

In addition to looking at the product distribution change upon altering the H_2/CO_2 ratio, the influence that pressure had on the reaction products at a fixed H_2/CO_2 ratio of 3:1 was considered. As the pressure was decreased from 450 to 150 psi, the rate of CO_2 and H_2 conversion was reduced from 41.18 to 4.67% (∼10-fold) and 50.55 to 10.55% (about 5-fold) (Table 3). It was observed in Table 4 that, with a drop in pressure, the selectivity shifted toward longer chain HCs and away from methane but the olefin selectivity became negligible as the pressure was reduced to 150 psig.

A lot of attention has been directed toward understanding the reaction mechanism of different metal surfaces in the FT synthesis. It has been shown that the mechanism is highly dependent upon the metal employed[20,21] and the differences in active site, i.e., stepped and flat surfaces.[22,23] Cobalt catalysts have shown chain-growth pathways to include $C + CH_3$ and $CH_2 + CH_2$, mainly taking place on the step sites for syngas. This reaction pathway is most likely the main contribution to C−C coupling in the FT process.[21] Looking at the traditional FT process reaction pathway and intermediates may help in understanding the processes involved in the hydrogenation of CO_2. The hydrogenation of CO_2 is stoichometrically defined by the following equations:

$$nCO_2 + (3n + 1)H_2 \rightarrow 2nH_2O + C_nH_{2n+2} \quad (2)$$

(for methane, $n = 1$; for longer chain HC paraffins, $n > 1$)

$$nCO_2 + 3nH_2 \rightarrow 2nH_2O + C_nH_{2n+2} \quad (3)$$

(for olefins)

As one can see, while the formation of methane requires a ratio of 4:1 H_2/CO_2 (with $n = 1$), the formation of longer chain HC actually needs a slightly lower H_2/CO_2 ratio of $(3n + 1):n$ (with $n > 1$) and an even lower ratio for CO_2 conversion to olefins (3:1). This mechanism, however, considers direct conversion of CO_2 rather than the conversion of CO_2 to CO via the WGS reaction with subsequent FT synthesis.

$$CO + H_2O \rightleftarrows CO_2 + H_2(WGS) \quad (4)$$

(20) Cheng, J.; Hu, P.; Ellis, P.; French, S.; Kelly, G.; Lok, C. M. *J. Phys. Chem. C* **2008**, *112*, 6082–6086.

Table 2. Product Distribution at 275 psi and 220 °C

ratio	TOS (h)	CH_4 (mol %)	C2= (mol %)	C2 (mol %)	C3= (mol %)	C3 (mol %)	C4= (mol %)	C4 (mol %)	CO
	226	97.6	0	1.5	0.1	0.5	0.1	0.2	0
	249	97.8	0	1.5	0	0.5	0	0.2	0
	278	97.7	0	1.5	0.1	0.5	0.1	0.2	0
3:1 H_2/CO_2	323	97.6	0	1.6	0.1	0.5	0.1	0.2	0
	346	97.7	0	1.6	0	0.5	0	0.2	0
	371	97.5	0	1.6	0.1	0.5	0.1	0.2	0
	393	97.6	0	1.6	0.1	0.5	0.1	0.2	0
	417	97.1	0	1.8	0	0.8	0	0.2	0
	444	97.1	0	1.9	0.1	0.7	0.1	0.2	0
2:1 H_2/CO_2	494	97.1	0	1.9	0	0.8	0	0.2	0
	514	96.8	0	2.0	0.1	0.8	0.1	0.3	0
	538	97.2	0	2.0	0	0.6	0	0.2	0
	753	94.9	0	2.1	0.2	2.1	0.3	0.5	0
	784	94.0	0	2.1	0.4	2.2	0.5	0.7	0
1:1 H_2/CO_2	836	93.7	0	2.4	0.3	2.6	0.2	0.6	0
	880	94.2	0	2.0	0.3	2.5	0.3	0.7	0
	1000	93.1	0	2.2	0.7	2.3	0.7	0.9	0

Table 3. Sample Conditions as a Function of Pressure at 220 °C and a H_2/CO_2 Ratio of 3:1

		feed in (SLPH)		feed out (SLPH)		conversion (%)	conversion (%)
pressure (psi)	TOS (h)	H_2	CO_2	H_2	CO_2	H_2	CO_2
	23	31.3	11.9	15.5	7.0	50.6	41.2
	75	31.3	11.9	15.9	7.1	49.3	40.1
450	90	32.4	11.9	16.1	7.4	48.6	37.5
	114	32.4	10.8	18.7	6.7	42.2	37.7
	120	32.4	10.8	19.1	6.9	41.1	36.4
	138	32.4	10.8	19.9	7.0	38.6	35.0
350	161	32.4	10.8	22.8	8.0	29.6	25.8
	211	32.4	10.8	25.2	8.7	22.2	19.3
	288	32.4	10.8	26.7	9.4	17.5	13.2
250	304	32.4	10.8	26.3	9.2	19.0	14.7
	328	32.4	10.8	27.1	9.4	16.4	12.7
150	378	32.4	10.8	28.9	10.4	10.8	3.5
	418	32.4	10.8	29.0	10.3	10.6	4.7

Table 4. Product Selectivity as a Function of Pressure at 220 °C and a H_2/CO_2 Ratio of 3:1

pressure (psi)	TOS (h)	CH_4 (mol %)	C2= (mol %)	C2 (mol %)	C3= (mol %)	C3 (mol %)	C4= (mol %)	C4 (mol %)
	23	96.9	0	1.8	0	0.9	0	0.4
	75	96.8	0	1.9	0	0.9	0	0.4
450	90	96.3	0	2.0	0	1.1	0	0.6
	114	97.2	0	1.8	0	0.8	0	0.3
	120	97.1	0	1.8	0	0.8	0	0.3
	138	97.1	0	1.9	0	0.8	0	0.3
350	161	96.9	0	2.1	0	0.8	0	0.3
	211	96.8	0	2.2	0	0.8	0	0.3
	288	96.5	0	2.5	0	0.7	0	0.3
250	304	96.6	0	2.5	0	0.7	0	0.2
	328	96.4	0	2.6	0	0.7	0	0.2
150	378	95.8	0	3.0	0	0.9	0	0.3
	418	95.7	0	3.3	0	0.8	0	0.3

Methane is the main reaction product when CO_2 is part of the feed gas. However, with increasing TOS, one can see a slight increase in CO_2 conversion to C_2-C_4 products (Table 2). An explanation of this occurrence may be a change in catalyst morphology; as the H_2/CO_2 consumption ratio adjusts to changes in the feed gas ratio, an overall constant consumption of the different feed gas components is observed. The catalyst is comprised of Pt and Co on a support, and it has been shown that the addition of Pt improves the CO hydrogenation rate without affecting the active sites of cobalt.[24] It is proposed that the Pt increases the hydrogenation rate of the cobalt by increasing the amount of cobalt being reduced.[24−26] With increasing TOS, the possibility arises of carbonaceous deposits forming an overlayer on parts of the catalyst,[27] which we can infer to be on the cobalt particles rather than the Pt, because of the role that cobalt plays in the CO_2 hydrogenation mechanism. These deposits seem to show a preference for certain active sites of the catalyst, i.e., stepped versus flat surfaces, leading to a decrease in the overall methanation ability of the catalyst and, thus, an increase in longer chain HC being formed in preference over methane. The step sites have shown to be the energetically more favorable sites for chain growth over the other sites in the FT process;[20] we may assume the same sites are responsible for chain growth in the hydrogenation of CO_2 to higher chain HC. The nature of the reaction products and the change in their distribution with increasing TOS indicates the presence of at least two different sites for CO_2 hydrogenation. It is thus feasible to deduce that the methane formation takes place on one specific surface, possibly the flat surface because this surface might show a preference for tripodal CO_2 adsorption,[28] with carbonaceous deposits showing a preference for this site and, thus, methane formation dropping with increasing TOS. The C−C coupling reaction site, possibly the step site, is most likely less affected by coking, which results in the increased fraction of C_2-C_4 products being formed. Further *in situ* studies on the morphology of the catalyst will have to be conducted to investigate these possibilities in more detail. The deactivation of certain active sites involved in methane formation, in favor of chain-growth sites, seems to play a role in the slight shift toward higher chain HC with increasing TOS, as can be inferred by the decreased fraction of methane being formed, as can be seen, for example, between 753 and 1000 h TOS.

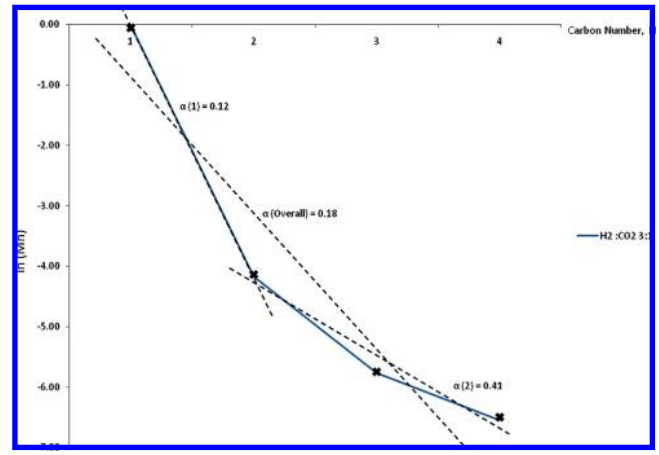

Figure 1. ASF distribution over the Co−Pt/Al_2O_3 catalyst at a H_2/CO_2 ratio of 3:1, showing a distinct break in the graph, thus, indicating two different growth sites resulting in α1 and α2. The dashed line is the fitted plot, which indicates the chain-growth probability, while the solid line is the actual data obtained from the catalyst.

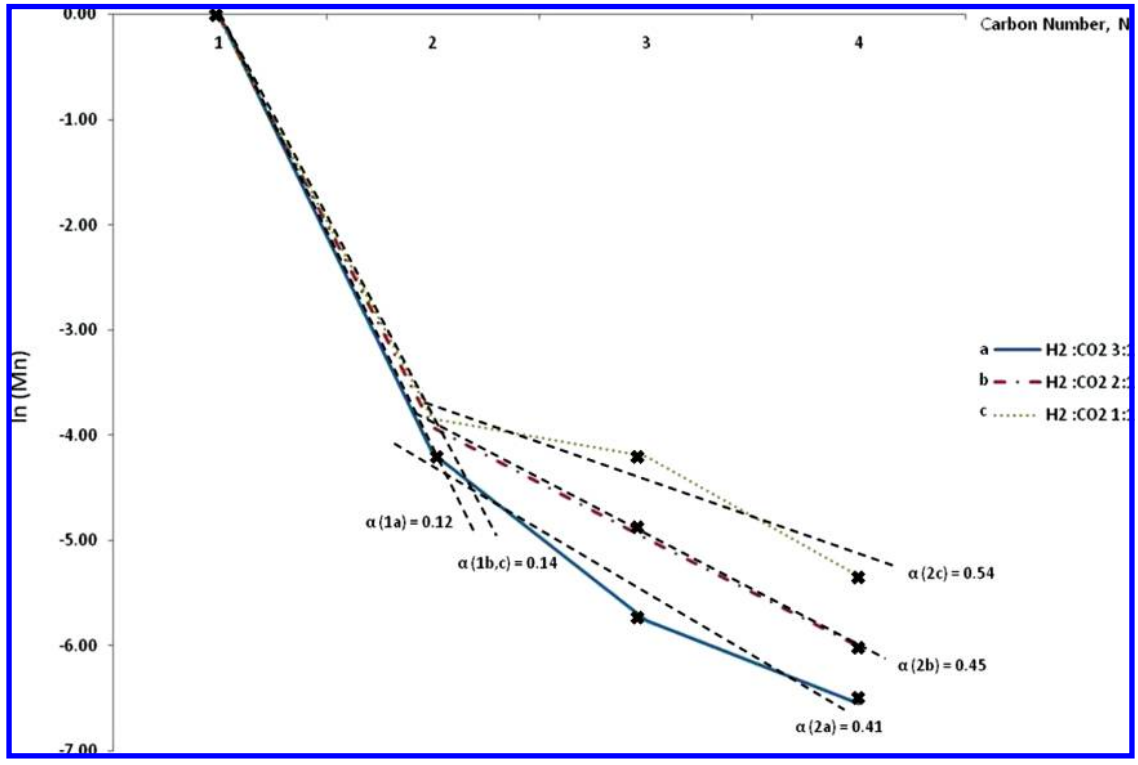

Figure 2. ASF distribution over the Co−Pt/Al_2O_3 catalyst at different H_2/CO_2 ratios [(a) 3:1, (b) 2:1, and (c) 1:1]. Chain-growth probability increases with a decreasing H_2/CO_2 ratio from (a) 0.41 to (c) 0.54. The dashed line is the fitted plot, which indicates the chain-growth probability, while the solid line is the actual data obtained from the catalyst, with the data points highlighted by an ×.

Furthermore, when looking at the redistribution of reaction products toward higher chain HC upon reducing the amount of hydrogen in the feed gas stream, the lack of CO present in the effluent (see Table 2), and the overall low WGS ability of co-catalysts,[29] we can infer a direct hydrogenation of CO_2 following the Langmuir−Hinshelwood mechanism.[30] It is highly unlikely that a two-step mechanism involving a reverse WGS function, i.e., following the Eley−Rideal mechanism,[31] is taking place, coupled with the FT chain-growth process, because one would expect to see CO as a product in the effluent because of partial CO dissociation from the metal surface.

Because no detailed *in situ* work has been conducted on chain-growth pathways, it is not possible to deduce if the reaction intermediates are identical to the ones formed over comparable co-catalysts in the FT process. However, because the fraction of C_2-C_4 olefins is extremely low, we can infer that most olefins produced are consumed in secondary side reactions upon readsorption on the chain-growth sites of the catalyst. This leads to long-chain hydrocarbon formation or direct hydrogenation. However, when the H_2 volume is lowered to equal the amount of CO_2 in the feed gas, we can infer that the accompanying rise in olefins is due to the lack of H_2 and, thus, olefin formation is preferred (see eqs 2 and 3). As stipulated earlier, the presence of several different active sites on this catalyst may be the cause for the high methane yield, because one active site favors methane formation in comparison to chain growth.[32,33] The product distribution may be furthermore controlled by the readsorption of olefins and subsequent incorporation into chain growth on the surface of the catalyst[34] and is probably the underlying reason for the distribution toward C_2-C_4 paraffin products and the lack of olefin products (especially ethene) during CO_2 hydrogenation.

Anderson−Schulz−Flury (ASF) plots seem to corroborate these findings. When plotting $\ln(M_N)$ against N (with M_N being the molar fraction of linear products with carbon number N), one expects to obtain a linear relationship, where α (i.e., chain-growth probability) can be obtained from the slope of the graph. When one obtains a break within the ASF distribution graph, two growth sites with different α values can be concluded.[35,36] Figure 1, which illustrates the ASF distribution over the catalyst (H_2/CO_2 ratio of 3:1), shows a clear break around the C_2 products, with α being 0.12 (α1) for the first and 0.41 (α2) for the second segment of the plot. When an average of the graph is taken, a value of 0.18 is obtained for α. Upon comparing the chain-growth probability obtained from the ASF plots at different H_2/CO_2 ratios, α2 increases with decreasing H_2 content in the feed gas, ranging from 0.41, 0.45, and 0.54 for the 3:1, 2:1, and 1:1 ratios, respectively (see Figure 2), highlighting the

(21) Lo, J. M. H.; Zeigler, T. *J. Phys. Chem. C* **2008**, *112*, 3692–3700.
(22) Ge, Q.; Neurock, M. *J. Phys. Chem. B* **2006**, *110*, 15368–15380.
(23) Cheng, J.; Gong, X.-Q.; Hu, P.; Lok, C. M.; Ellis, P.; French, S. *J. Catal.* **2008**, *254*, 285–295.
(24) Vada, S.; Hoff, A.; Adnanes, E.; Schanke, D.; Holmen, A. *Top. Catal.* **1995**, *2*, 155–162.
(25) Das, T. K.; Jacobs, G.; Davis, B. H. *Catal. Lett.* **2005**, *101*, 187–190.
(26) Batley, G. E.; Ekstrom, A.; Johnson, D. A. *J. Catal.* **1974**, *34*, 368–375.
(27) Rossi, S. D.; Ferraris, G.; Fermiotti, S.; Cimino, A.; Indovina, V. *Appl. Catal., A* **1992**, *81*, 113–132.
(28) Hammami, R.; Dhouib, A.; Fernandez, S.; Minot, C. *Catal. Today* **2008**, *139*, 227–233.
(29) Khodakov, A. Y.; Chu, W.; Fongarland, P. *Chem. Rev.* **2007**, *107*, 1692–1744.
(30) Maitlis, P. M.; Quyoum, R.; Long, H. C.; Turner, M. L. *Appl. Catal., A* **1999**, *186*, 363–374.
(31) Jakdetchai, O.; Nakajima, T. *J. Mol. Struct.* **2002**, *619*, 51–58.
(32) Ponec, V. *Catal. Rev. Sci. Eng.* **1978**, *18*, 151–171.
(33) Schulz, H. *Appl. Catal., A* **1999**, *186*, 3–12.
(34) Kuipers, E. W.; Scheper, C.; Wilson, J. H.; Vinkenburg, I. H.; Oosterbeck, H. *J. Catal.* **1996**, *158*, 288–300.
(35) Patzlaff, J.; Liu, Y.; Graffmann, C.; Gaube, J. *Appl. Catal., A* **1999**, *186*, 109–119.
(36) Schulz, H.; Claeys, M. *Appl. Catal., A* **1999**, *186*, 91–107.

shift from methane toward longer chain HC with a decreasing H_2/CO_2 ratio. A clear break between methane and any longer chain hydrocarbons of this magnitude would be very unusual for typical ASF plots of the FTS process. Thus, such a distinction found in this study highlights the fact that the Co-catalyst is not behaving as a FTS catalyst but, instead, as a methanation catalyst in CO_2 hydrogenation.

All of the data show the same trend with two α values obtained over the range of the plot. This finding is in good agreement with previously stated conclusions in this work and points toward two different active sites for methane and C_2-C_4 formation. However, only at the H_2/CO_2 ratio of 1:1 do we see the common drop in C_2 products in the ASF distribution curve, while at all other reactant ratios, this is not observed (see Figure 2). Interestingly, at this ratio, we also obtain the highest long change HC selectivity, indicating that chain growth occurs at the expense of ethane (and possibly ethene if formed).

4. Conclusions

The need for alternative energy sources is becoming ever more important with the rising costs of crude oil and the inevitable reality of peak oil. The recycling of environmental CO_2 by subsequent conversion to fuel would result in neutral CO_2 emissions by the fuel. This would not only be of interest based on the cost of CO_2, but it would also reduce the impact it has on global warming. CO_2, however, has been shown very little attention by industry and academia because of its high thermodynamic stability. This study shows the conversion of CO_2 to predominantly methane with a small fraction of longer chain HC being formed in the C_2-C_4 product range. Reducing the feed gas ratio of H_2/CO_2 from 3:1 to 2:1 and subsequently to 1:1 and lowering the operating pressure has led to the modification of the product distribution toward longer chain HC, i.e., a reduction in methane formation. Additionally, deactivation of the methane-forming active sites with increasing TOS seems to play a role in the product distribution shift toward C_2-C_4 HC, as can be seen by the reduced methane production with increasing TOS, irrespective of the feed gas ratio. It is speculated that the change in the feed gas ratio leads to a lowering of the catalyst's methanation ability of CO_2 in favor of chain growth, with two different active sites for methane and C_2-C_4 products present on the surface of the catalyst. Future research will be directed toward determining the proposed reaction mechanism and corroborate the hypotheses.

Acknowledgment. This work was supported by the Office of Naval Research both directly and through the Naval Research Laboratory.

EF900275M